https://doi.org/10.5194/egusphere-2026-6718
Preprint. Discussion started: 16 November 2026
© Author(s) 2026. CC BY 4.0 License.

Methane Distribution in the East (Japan) Sea: Baseline for Donghae Gas Field Carbon Storage Project

Junyoung Lee[1], Seungryong Baek[2], Eun-Hee Lee[2,3], Doshik Hahm[1], Intae Kim[4], Boo-Keun Khim[1], Janghan Lee[3] and DongJoo Joung[1,3*]

[1]Department of Oceanography, Pusan National University, Busan, Republic of Korea.
[2]Department of Microbiology, Pusan National University, Busan, Republic of Korea.
[3]Institute for Future Earth, Pusan National University, Busan, Republic of Korea.
[4]Marine Environmental Research Center, Korea Institute of Ocean Science and Technology, Busan, Republic of Korea.
Correspondence to: DongJoo Joung (dongjoo.joung@pusan.ac.kr)

Abstract. Methane (CH_4), the second most potent greenhouse gas, is poorly characterized in coastal waters along the Korean Peninsula. We investigated dissolved CH_4 across depths and distances from shore in the southwestern East (Japan) Sea (EJS) and the adjacent Ulleung Basin. Concentrations ranged from 1.7 to 48.7 nM, with maxima near the coast and seafloor, though the mixed layer held the maximum at some stations. Bottom-water CH_4 (1.7–28.2 nM, mean: 7.0 ± 4.5 nM, n = 44) was 2- to 10-fold higher than surface water (2.0–4.4 nM, mean: 3.2 ± 0.6 nM, n = 48), consistent with a sedimentary source typical of shallow continental shelves. In the Ulleung Basin, however, the CH_4 maximum occurred in the mixed layer, likely reflecting stratification-driven microbial production and possible lateral advection. CH_4 declined from coast to offshore along a consistent density layer in October 2025, suggesting lateral transport to the open ocean. Sea-to-air CH_4 flux from the southwestern EJS ranged from −2.1 to 35.6 μmol m^{-2} d^{-1} (mean: 8.6 ± 10.6 μmol m^{-2} d^{-1}), comparable to other global continental margins, with greater release in warm seasons. Given ongoing warming in the EJS, atmospheric CH_4 emissions may increase further. Several stations lie within the Donghae gas field, a depleted reservoir considered for CO_2 storage; CH_4 there (7–10 nM) matched regional background, providing a pre-injection baseline for future leakage monitoring. This is the first multi-season water-column CH_4 dataset for this sector of the Korean coast, though CH_4 sources remain poorly constrained.

Keywords: Methane (CH_4), Lateral advection, Sea-to-air flux, East (Japan) Sea, Donghae gas field, Carbon capture and storage

1 Introduction

Methane (CH_4) is the second most abundant anthropogenic greenhouse gas in the atmosphere after carbon dioxide (CO_2) and plays a crucial role in the Earth's climate system (Lashof and Ahuja, 1990). Although the atmospheric mixing ratio of CH_4 (1.93 ppm) is about 1/200 that of CO_2 (423 ppm) (Lan et al., 2025), CH_4 accounts for ~17% of global warming, representing the second-largest contribution among greenhouse gases (IPCC, 2021). The global mean atmospheric CH_4 mixing ratio reached approximately 1931 ppb in 2025, representing an increase of more than 160% relative to the pre-industrial level (729 ppb) in 1750 and exhibits a pronounced long-term increasing trend (IPCC, 2021; Lan et al., 2025). This rising is primarily attributed

https://doi.org/10.5194/egusphere-2026-6718
Preprint. Discussion started: 16 November 2026
© Author(s) 2026. CC BY 4.0 License.

to anthropogenic sources, that is, emissions caused by direct human activities (e.g., agriculture and fossil fuel use) (Saunois et al., 2019).

Marine systems (e.g., estuaries, coastal waters, and the open ocean) constitute one of the natural sources of CH_4 to the atmosphere (Reeburgh, 2007). Estimates suggest that marine CH_4 emissions are approximately 5–25 Tg CH_4 yr^{-1}, accounting for about 1–13% of total natural CH_4 emissions (Saunois et al., 2016). The distributions and emissions of CH_4 in the ocean exhibit strong variability upon systems such as estuaries (~7 Tg CH_4 yr^{-1}), coastal regions (~13 Tg CH_4 yr^{-1}), and the open ocean (0.4–1.2 Tg CH_4 yr^{-1}) (Bates et al., 1996; Rhee et al., 2009; Borges et al., 2016; Sun et al., 2018). Among these, the coastal seas play a significant role in marine CH_4 emissions; although they occupy only a small proportion of the global ocean area, they account for roughly 75% of the total marine CH_4 emissions (Bange et al., 1994; Hamdan et al., 2016). These relatively high CH_4 concentrations in coastal waters compared to the open ocean are generally attributed to riverine inputs, sediment release, and hydrocarbon seeps particularly in nearshore regions with shallow water depths (Upstill-Goddard et al., 2000; Reeburgh, 2007; Zhang et al., 2008; Borges et al., 2016).

In coastal environments without major rivers, CH_4 in the water is mainly sourced from sediments and the hydrocarbon seeps via diffusion and/or bubble transport (e.g., Gulf of Mexico) (Solomon et al., 2009; Joung et al., 2025). Within sediments the organic matter is decomposed and, at the final stage of the decomposition, CH_4 is generated through anaerobic methanogenesis. Thus, the production of CH_4 in this pathway could largely be impacted by microbial activity and organic matter supply (Reeburgh, 2007). As such, coastal eutrophication would lead to an increase in CH_4 production in coastal waters. In general, coastal eutrophication drives a rapid increase in primary production, and eventually the organic matter is deposited to the seafloor, thereby decomposing while consuming oxygen. When this process persists, sediments become hypoxic or even anoxic, enhancing CH_4 release to the water column and to the atmosphere (Rabalais et al., 1991; Turner et al., 2006; Reeburgh, 2007; Gelesh et al., 2016; Bange et al., 2018). Furthermore, many recent studies have indicated that coastal eutrophication and associated hypoxic events, driven by progressing ocean warming, are projected to increase in both duration and spatial extent (Stramma et al., 2008; Breitburg et al., 2018). This trend will enhance CH_4 accumulation in the water column and its emission to the atmosphere, thereby amplifying climate warming and potentially forming a positive feedback loop in the climate system (Saunois et al., 2016; Ruppel and Kessler, 2017).

Although CH_4 is produced mainly in sediments, most of CH_4 is anaerobically oxidized at the sulfate-methane transition zone (SMTZ) by donating electrons for sulfate reduction during its upward migration (Reeburgh, 2007). Therefore, the actual CH_4 release to the water column can be lower than the sedimentary production (Reeburgh, 2007), though it is still much greater than production within the water column. Once released to the water column and transported to the upper water column via diffusion or bubble transport, CH_4 would also be removed through aerobic oxidation within the water column (Kastner, 2001; Valentine, 2001; Leonte et al., 2018). This means that, in oxygenated aquatic environments, the overall sedimentary CH_4 emission to the water column and to the atmosphere would be substantially decreased during upward migration. For example, Żygadłowska et al. (2024) found that the benthic CH_4 releases were in the range of 2.2–8.6 mmol m^{-2} d^{-1}, while atmospheric releases were only 0.1–1.7 mmol m^{-2} d^{-1}, indicating that up to 90% sedimentary CH_4 can be removed

https://doi.org/10.5194/egusphere-2026-6718
Preprint. Discussion started: 16 November 2026
© Author(s) 2026. CC BY 4.0 License.

within the water columns in Stockholm Archipelago. In general, the aerobic CH_4 oxidation is largely impacted by oxygen conditions, displaying lower oxidation rates when oxygen is unavailable (Steinle et al., 2017). Therefore, the estuarine CH_4 dynamics (i.e., sources and sinks) exhibit high spatiotemporal variability, leaving coastal CH_4 dynamics poorly understood (Saunois et al., 2016; IPCC, 2021). Hence, a more comprehensive understanding of oceanic CH_4 processes requires region-specific investigations and long-term observational efforts across diverse marine environments. In particular, dissolved CH_4 in coastal waters along the Korean coast has not been well-studied.

In this study, we examined CH_4 dynamics in waters from the EJS encompassing various water depths from shallow to deep ocean sites. The EJS is a semi-enclosed marginal sea in which water depth increases rapidly from the coastal zone to the open basin. The EJS is characterized by a high export of organic matter to depth and is known to contain abundant natural gas and gas hydrates, likely promoting CH_4 release to the water column (Huh et al., 2004; Kim et al., 2009; Kwon et al., 2011). Gamo et al. (2012) investigated vertical CH_4 distributions in major basins of the EJS (the Ulleung, Yamato, and Japan Basins) and showed that the observed vertical profiles were influenced by multiple biogeochemical processes, including in situ microbial production in the subsurface water column, inputs from seafloor sediments, and submarine seepage. However, the temporal and spatial resolutions of CH_4 dynamics in the EJS remain insufficient.

This study aimed to characterize the distribution of dissolved CH_4 in the EJS, covering various locations with different water depths, ranging from shallow coastal waters in the southwestern margin to deep sites in the Ulleung Basin. In addition, we estimated sea-to-air CH_4 fluxes and compared them with other regions to assess the relative contribution of the EJS to the global atmospheric CH_4 emissions. By providing new CH_4 observations in the EJS, this study would improve our understanding of marine CH_4 biogeochemical cycling along the Korean coast.

2 MATERIALS AND METHODS

2.1 Experimental Design

We investigated CH_4 dissolved in seawater from the southwestern EJS and the Ulleung Basin during five sampling cruises: July 2023, April 2024 (R/V *Onnuri*), March 2025 (R/V *Isabu*), June 2025 (R/V *Dokdonuri*), and October 2025 (R/V *Onnuri*). To investigate the spatiotemporal variability of dissolved methane CH_4 concentrations and sea-to-air CH_4 fluxes in the southwestern East/Japan Sea (EJS) and the Ulleung Basin, a comprehensive observational and analytical approach was established (Fig. 1). The overall experimental design and workflow are summarized in Fig. 2. Briefly, seawater samples and ancillary environmental data (temperature, salinity, and dissolved oxygen) were collected across five field cruises between July 2023 and October 2025. Dissolved CH_4 was extracted via headspace equilibration and quantified using gas chromatography with a flame-ionization detector (GC-FID) to compute sea-to-air fluxes. In addition, selected seawater samples were processed for genomic DNA extraction and quantitative real-time PCR (qPCR) to assess bacterial abundances.

https://doi.org/10.5194/egusphere-2026-6718
Preprint. Discussion started: 16 November 2026
© Author(s) 2026. CC BY 4.0 License.

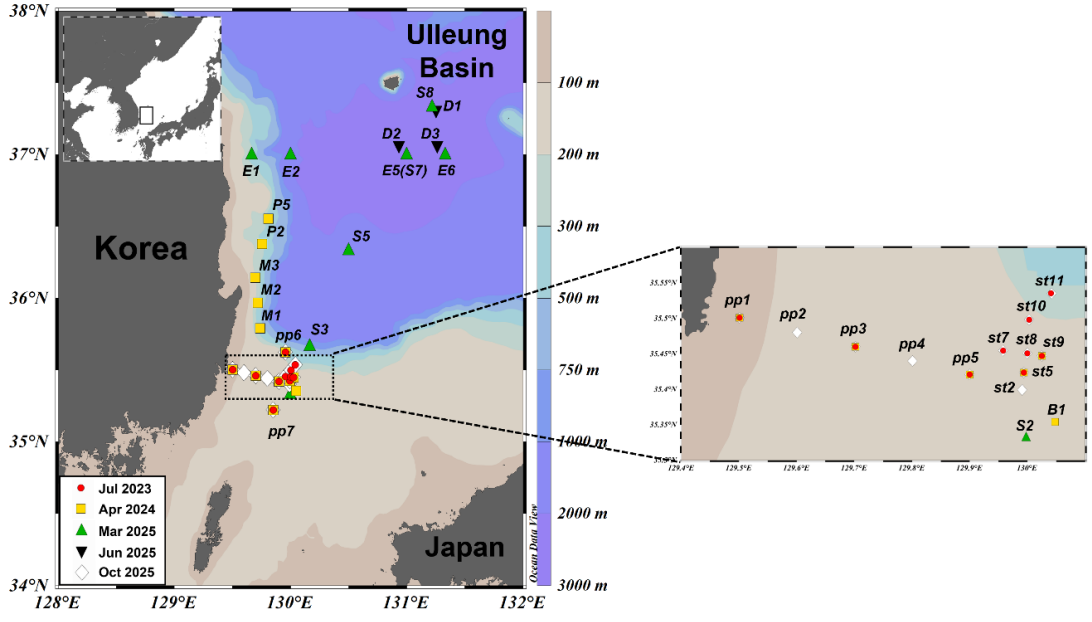


Figure 1. Map of bathymetry and sampling stations in the southwestern EJS, including the Ulleung Basin. Red circles, yellow squares, green triangles, black inverted triangles, and white diamonds represent stations from the July 2023, April 2024, March 2025, June 2025, and October 2025 cruises, respectively.

https://doi.org/10.5194/egusphere-2026-6718
Preprint. Discussion started: 16 November 2026
© Author(s) 2026. CC BY 4.0 License.

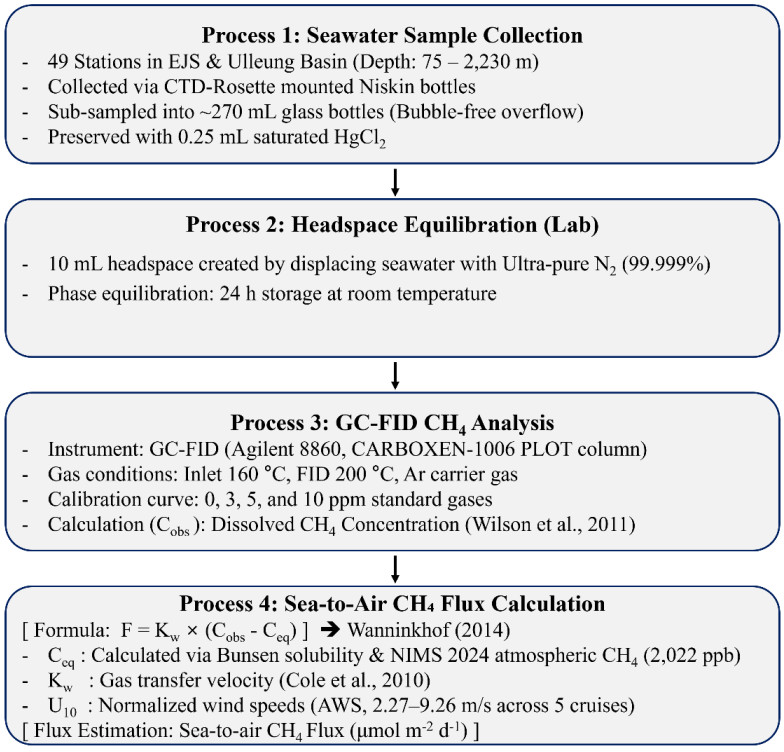


Figure 2. Detailed flowchart showing the step-by-step procedures for CH_4 analysis and flux estimation: Step 1, seawater sampling and $HgCl_2$ preservation; Step 2, laboratory headspace equilibration; Step 3, quantification of dissolved CH_4 concentration using GC-FID; and Step 4, determination of sea-to-air CH_4 flux with meteorological and solubility data.

2.2 Study area

The EJS is a semi-enclosed basin surrounded by Korea, Russia, and Japan. The EJS is often referred to as a "miniature ocean" because it exhibits a meridional overturning circulation similar in structure to that of the open ocean, with a timescale of ~100 years—substantially shorter than the ~1,000-year timescale typical of the open ocean (Lee and Rho, 2015). The southwestern EJS is influenced by the warm, saline Tsushima Warm Current—a branch of the Kuroshio Current that enters through the Korea Strait—as well as by the cold, fresh, and low-salinity North Korea Cold Current that flows southward along the coast (Byun and Chang, 1984; Chang et al., 2004). The region is also characterized by active seasonal coastal upwelling and freshwater discharge, primarily from the Nakdong River, along the coast, leading to pronounced spatiotemporal environmental variability (Won and Lee, 2015). The inner shelf is characterized by a thick Holocene mud layer formed by alongshore transport and deposition of fine-grained sediments derived from the Nakdong River; radiocarbon aging of piston-core sediments indicates that these mud deposits have accumulated over the past 4.9 ka (Chun et al., 2015). The EJS comprises three major

https://doi.org/10.5194/egusphere-2026-6718
Preprint. Discussion started: 16 November 2026
© Author(s) 2026. CC BY 4.0 License.

basins (the Ulleung, Yamato, and Japan Basins), among which the Ulleung Basin is directly fluenced by the Tsushima Warm Current. This current delivers organic matter and nutrients derived from the Nakdong River, thereby fueling primary production alongside the atmospheric deposition (Takata et al., 2008; Shim and Yoon, 2021).

2.3 Seawater collection

The CH_4 samples were collected from a total of 49 stations, with various seafloor depths ranging from 75 m (Stn. pp1) to 2,230 m (Stn. S8; Ulleung Basin) (Fig. 1). Seawater samples were collected from Niskin bottles mounted on the CTD rosette sampler. Once the Niskin bottles were recovered, water samples for dissolved CH_4 were collected in a glass bottle (~270 mL) using a silicone tube, allowing two to three bottles volume to overflow to minimize bubble entrapment. Immediately after sampling, each bottle was sealed with a butyl rubber stopper and an aluminum crimp cap. In the laboratory, 0.25 mL of a saturated mercuric chloride ($HgCl_2$) solution was added to inhibit microbial activity, after which the sample bottles were brought back to the land-based laboratory (Weinstein et al., 2016). Triplicate samples were collected at each depth. Microbial biomass was also determined during limited sample collection in March and June 2025. For the microbial biomass, unfiltered seawater samples were collected in sterile 1 L low-density polyethylene (LDPE) sample bags (Winners, Korea) and stored in a refrigerator with temperature set to 4 °C.

2.4 Methane analysis

Dissolved CH_4 concentrations were determined using the headspace equilibration method (Upstill-Goddard et al., 1996). A 10-mL headspace was created in each ~270-mL bottle by displacing a portion of seawater with ultra-pure nitrogen (N_2, 99.999%) gas. The bottles were then inverted and allowed to equilibrate at room temperature for 24 h to ensure phase equilibrium between the headspace and the seawater. Headspace gas was analyzed using a gas chromatograph (GC 8860; Agilent, USA) equipped with a flame-ionization detector (FID). Samples were injected into an inlet maintained at 160 °C, and CH_4 separation was achieved using a CARBOXEN-1006 PLOT column (30-m length) with argon (Ar) as the carrier gas. The FID was operated at 200 °C, using ultra-high-purity hydrogen (H_2, 99.999%) and air (99.999%) as fuel and oxidant gases, respectively. Dissolved CH_4 concentrations were determined based on a calibration curve established using standard gases (0, 3, 5, and 10 ppm) during each analysis run. The final concentrations in the sample bottles were then calculated according to the equations described by Wilson et al. (2018).

Ancillary data, including temperature, salinity, and dissolved oxygen, were obtained using a shipboard conductivity-temperature-depth (CTD) and a dissolved oxygen sensor (SeaBird 911) equipped on the rosette system, and sample collection depths for CH_4 were determined after examining profiles of the ancillary data.

https://doi.org/10.5194/egusphere-2026-6718
Preprint. Discussion started: 16 November 2026
© Author(s) 2026. CC BY 4.0 License.

2.5 Methane sea-to-air flux calculations

The atmospheric flux (F, μmol m^{-2} d^{-1}) of CH_4 was estimated following Wanninkhof (1992):

$$F = K_w \times (C_{obs} - C_{eq}) \quad (1)$$

where C_{obs} is the observed dissolved CH_4 concentration, C_{eq} is the equilibrium concentration with the atmosphere, and K_w is the gas transfer velocity. Following Wanninkhof (1992), C_{eq} was calculated using the Bunsen solubility coefficient and the atmospheric partial pressure of CH_4. Because atmospheric CH_4 concentrations were not measured in situ during this study, we utilized the 2024 annual mean atmospheric CH_4 value of 2,022 ppb measured at the Ulleungdo monitoring station, obtained from the National Institute of Meteorological Sciences (NIMS) Report of Global Atmosphere Watch (NIMS, 2024). The gas transfer velocity (K_w), which is mainly controlled by the wind speed, was calculated following Cole and Caraco (1998). The wind speeds measured by the shipboard automatic weather system (AWS) were normalized to a height of 10 m above the sea surface (U_{10}) prior to calculation of K_w. The cruise-averaged U_{10} wind speeds were measured by a ship-mounted weather station and were 7.01, 2.27, 5.44, 4.40, and 9.26 m s^{-1} for cruises of July 2023, April 2024, March 2025, June 2025, and October 2025, respectively.

2.6 Bacterial abundance analysis

Bacterial abundance was quantified by qPCR targeting the 16S rRNA gene. Seawater samples were filtered through cellulose acetate membrane filters (0.45 μm pore size, 47 mm diameter; Hyundai Micro, Korea). Genomic DNA was extracted from the membrane filters using a NucleoSpin Soil Kit (Macherey-Nagel GmbH, Düren, Germany) with minor modifications (Soliman et al., 2017). The extracted DNA was eluted in 60 μL of elution buffer, and DNA concentrations were determined using a NanoDrop 2000 spectrophotometer (Thermo Fisher Scientific, Waltham, MA, USA).

The bacterial 16S rRNA gene was amplified using primers 340F (5′-TCCTACGGGAGGCAGCAG-3′) and 805R (5′-GACTACHVGGGTATCTAATCC-3′) (Jeong and Kim, 2022). Each 20-μL qPCR reaction contained 10 μL of 2 × SYBR qPCR Master Mix (Toyobo Co., Ltd., Osaka, Japan), 0.6 μL of forward primer (10 μM), 1.2 μL of reverse primer (10 μM), 1 μL of template DNA, and nuclease-free water. Amplification was performed using an Applied Biosystems StepOne Real-Time PCR System (Thermo Fisher Scientific) under the following conditions: 95 °C for 30 s, followed by 40 cycles of 95 °C for 5 s, 50 °C for 10 s, and 72 °C for 60 s.

For construction of the qPCR standard curve, the 16S rRNA gene was amplified from Escherichia coli genomic DNA using the same primer pair. The resulting PCR product was purified using FavorPrepTM Gel/PCR Purification Mini Kit (FAVORGEN Biotech Corp., Ping Tung, Taiwan), and its DNA concentration was determined using a NanoDrop 2000 spectrophotometer. The copy number of the purified 16S rRNA gene amplicon was calculated based on its DNA concentration and amplicon length, and serial dilutions of the purified amplicon were used to generate the standard curve. Bacterial 16S rRNA gene abundance was determined from the standard curve based on the threshold cycle (C_t) values and expressed as gene

https://doi.org/10.5194/egusphere-2026-6718
Preprint. Discussion started: 16 November 2026
© Author(s) 2026. CC BY 4.0 License.

copies L^{-1} of seawater after accounting for the template dilution factor, DNA elution volume, and the volume of seawater filtered.

3 Results and Discussion

Surface dissolved CH_4 concentrations in the southwestern EJS ranged from 2.0–4.4 nM (mean: 2.9 ± 0.7 nM, n = 11), 2.7–3.7 nM (mean: 3.0 ± 0.3 nM, n = 13), and 2.5–4.4 nM (mean: 3.5 ± 0.6 nM, n = 13) in July 2023, April 2024, and October 2025, respectively (Figs. 3A–C; Tables S1–S3). In contrast, bottom water concentrations were consistently and substantially higher, ranging from 3.7 to 11.4 nM (mean: 6.9 ± 2.5 nM, n = 11), 3.8–14.2 nM (mean: 7.3 ± 3.2 nM, n = 12), and 3.8–28.2 nM (mean: 8.8 ± 6.1 nM, n = 14) during the same respective cruises (Figs. 4A–C; Tables S1–S3). Surface CH_4 concentrations in the Ulleung Basin (2.8–4.4 nM; Figs. 3D and E) were comparable to those in the southwestern EJS (Figs. 3A–C), despite its greater distance from land and distinct physiographic setting (Table S4). This spatial similarity in surface CH_4 levels between the southwestern EJS and the Ulleung basin, despite their differing proximity to the shore, indicates that terrestrial CH_4 inputs are confined to the immediate coastal margin and do not extend into the open surface layer of either basin. We note that the number of stations for averaging are uneven across cruises (ranging from n = 45–48 for the pooled surface/bottom datasets down to as few as n = 2 for some individual gas-field surveys); comparisons involving the smaller subsets should be read as indicative rather than statistically robust.

https://doi.org/10.5194/egusphere-2026-6718
Preprint. Discussion started: 16 November 2026
© Author(s) 2026. CC BY 4.0 License.

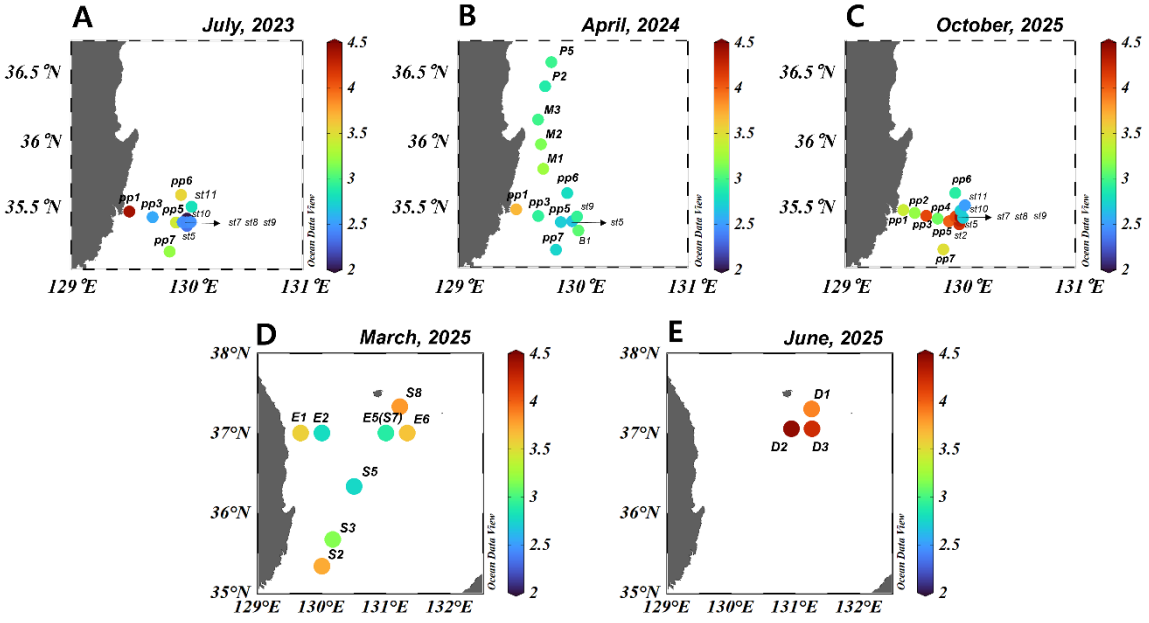


Figure 3. Spatial distributions of dissolved methane (CH_4) concentrations in surface waters of the southwestern East (Japan) Sea in (A) July 2023, (B) April 2024, and (C) October 2025, and of the Ulleung Basin during (D) March 2025 and (E) June 2025.

https://doi.org/10.5194/egusphere-2026-6718
Preprint. Discussion started: 16 November 2026
© Author(s) 2026. CC BY 4.0 License.

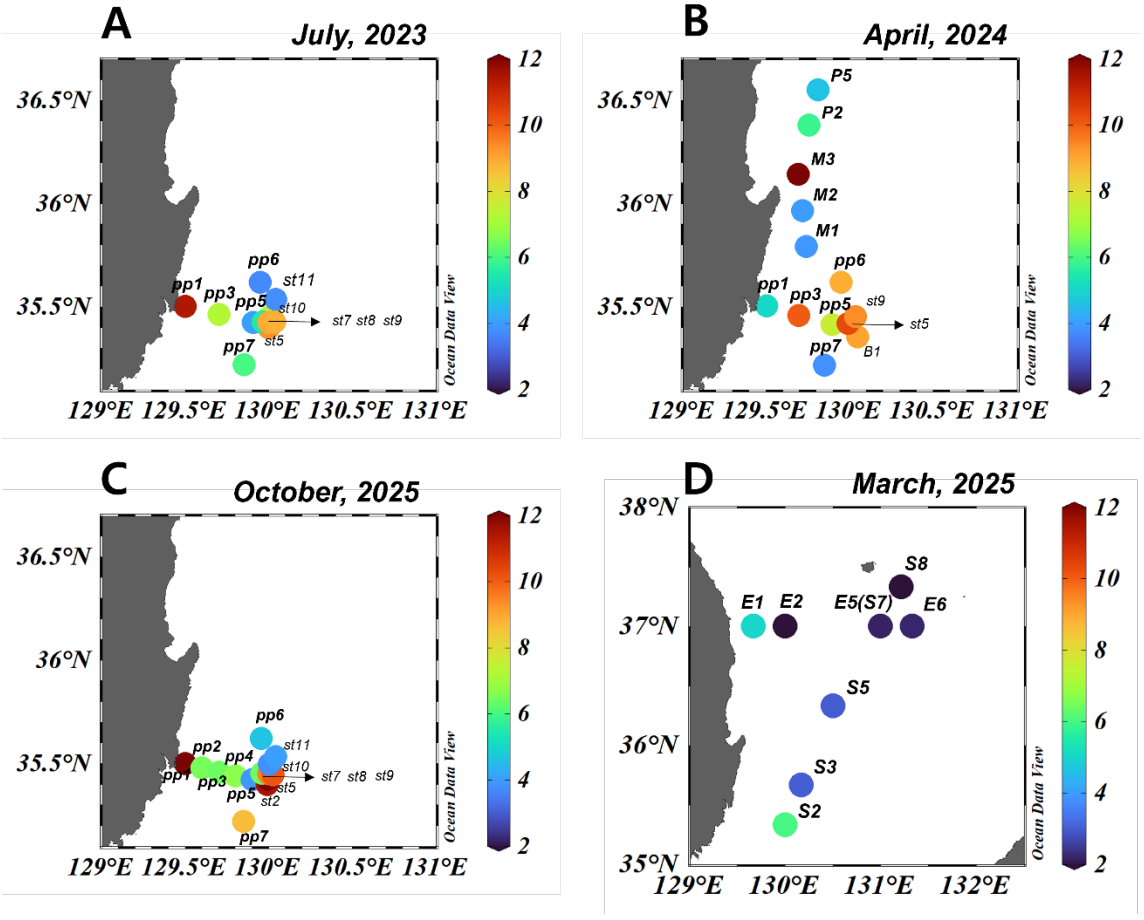


Figure 4. Spatial distributions of dissolved methane (CH_4) concentrations in bottom waters of the southwestern East (Japan) Sea in (A) July 2023, (B) April 2024, and (C) October 2025, and of the Ulleung Basin during (D) March 2025.

During all the three sample collection campaigns, there were no considerable variations in surface water CH_4 distribution (Fig. 3). The absence of a consistent interannual trend in surface CH_4 in the southwestern EJS across the three sampling years suggests that the CH_4 distribution in this system has remained relatively stable, with similar sources and sinks, over time. Vertically, both southwestern and Ulleung Basin in the EJS showed the expected CH_4 structure, displaying supersaturation in the surface water, a peak at the bottom of mixed layer corresponding to a subsurface oxygen minimum, and elevated concentrations near the seafloor (Figs. 5 and 6; Tables S1–S4). We note that the source attributions developed below (e.g., methylphosphonate degradation, benthic diffusion, lateral advection) rely on indirect physical and biogeochemical proxies—water-mass properties, oxygen and density structure, and microbial abundance—rather than on direct source tracers such as

https://doi.org/10.5194/egusphere-2026-6718
Preprint. Discussion started: 16 November 2026
© Author(s) 2026. CC BY 4.0 License.

CH_4 stable isotopes or methanogen-specific assays. Therefore, these interpretations should accordingly be read as the most plausible explanations consistent with our observations rather than as definitively established mechanisms.

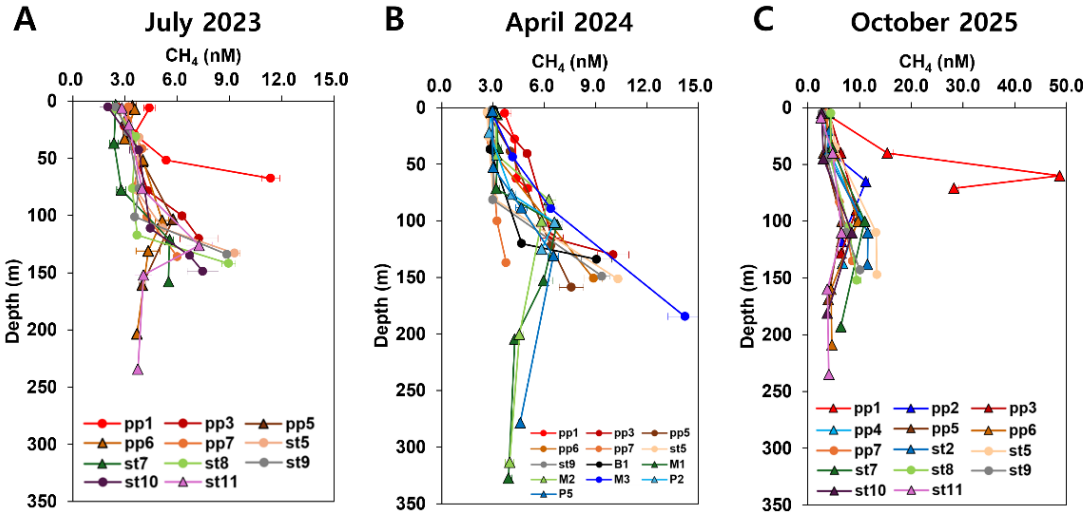


Figure 5. Vertical distributions of dissolved methane (CH_4) concentrations in the southwestern East (Japan) Sea in (A) July 2023, (B) April 2024, and (C) October 2025. Error bars indicate standard deviations at each observation depth (n = 2 for July 2023; n = 3 for April 2024 and October 2025).

https://doi.org/10.5194/egusphere-2026-6718
Preprint. Discussion started: 16 November 2026
© Author(s) 2026. CC BY 4.0 License.

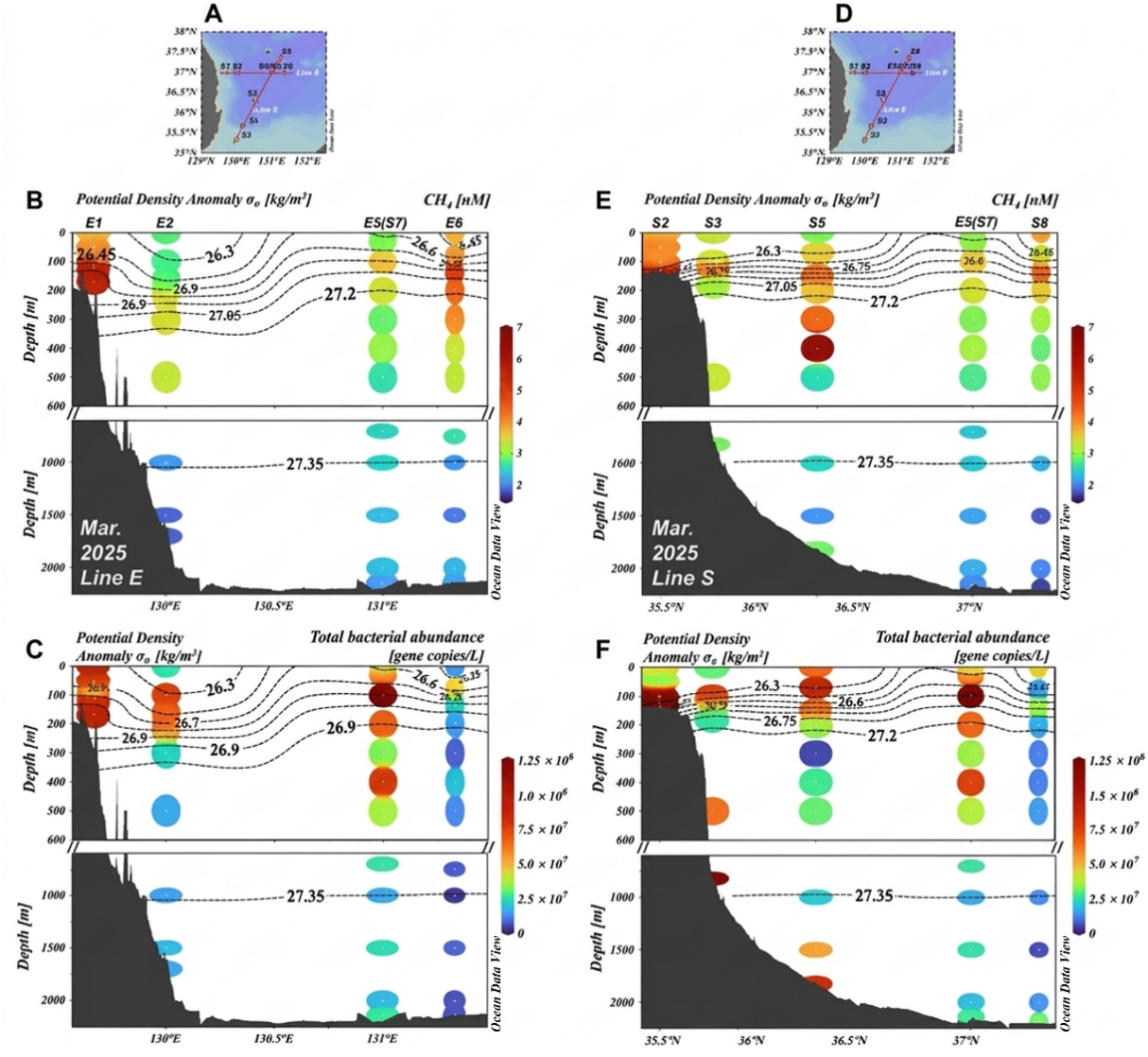


Figure 6. Vertical distributions of dissolved methane (CH_4) concentration and total bacterial abundance along vertical sections in the Ulleung Basin during March 2025. (A–C) Line E and (D–F) Line S transects, showing (A, D) sampling station locations, (B, E) CH_4 concentration (nM), and (C, F) total bacterial abundance (gene copies/L). Dashed contours indicate potential density anomaly (σ_θ, kg/m^3). Note that the vertical axis is broken to separate upper (0–600 m) and deep (600–2,250 m) water columns.

3.1 Mechanisms controlling surface CH_4 supersaturation

Surface waters at both sites were supersaturated with respect to atmospheric equilibrium (up to 200% saturation; Fig. S1G–H), consistent with the well-documented "ocean methane paradox". In this process, the aerobic microbial degradation of

https://doi.org/10.5194/egusphere-2026-6718
Preprint. Discussion started: 16 November 2026
© Author(s) 2026. CC BY 4.0 License.

methylphosphonate under phosphate limitation generates CH_4 as a byproduct (Karl and Tilbrook, 1994; Karl et al., 2008; Repeta et al., 2016; Zindler et al., 2013; Ye et al., 2025). Although nutrients were not directly investigated in this study, the surface waters at both sites have been reported to be highly depleted in phosphate (Lee et al., 2025), suggesting that observed CH_4 supersaturation could be associated with methylphosphonate degradation. However, this mechanism alone typically accounts for only a few percent supersaturation, even in extremely oligotrophic open-ocean settings (Reeburgh, 2007; Repeta et al., 2016), implying that an additional source is required to explain our observations.

Because of the proximity to the shore, freshwater input (e.g., Nakdong River) could potentially influence the study area. However, although the Nakdong River water can carry very high CH_4 concentrations (28 to >200 nM across salinities of 0–31; Lee et al., 2025), salinity at our study sites remained consistently above 32 across all surveys (Figs. S1D–F). Furthermore, stations closer to the river mouth did not show elevated CH_4 concentrations relative to those further offshore. In addition, surface salinity exhibited considerably more pronounced seasonal variations (32–34, lowest in July) than surface CH_4 did; notably, the July survey—which recorded the lowest salinity—did not show the highest CH_4 concentrations (Table S1 to S3). This decoupling suggests that the contribution of riverine input to surface CH_4 supersaturation could be limited. Therefore, freshwater input is unlikely to contribute significantly to the observed surface CH_4 supersaturation. Instead, both study regions are known sites of upwelling and mesoscale eddy activity (Kim et al., 2023). Particularly in the Ulleung Basin, seasonal water-mass replacement (Tsushima Warm Current in June vs. North Korea Cold Water in March; Kim et al., 2004; Lee et al., 2024) is accompanied by near-identical salinity but markedly different temperature. This indicates that distinct water masses, and by extension distinct eddy-driven upwelling regimes, plausibly modulate the seasonal surface CH_4 signal, although we did not characterize the CH_4 endmember of each water mass directly. In addition, both sites showed a slight surface dissolved-oxygen deficit relative to expected saturation, which is suggestive of intermittent upwelling of subsurface water and thereby CH_4 supply from the mixed layer.

3.2 Benthic input to bottom-water CH_4 in the southwestern EJS

The strong bottom-ward increase in CH_4 concentrations in the southwestern EJS indicates a significant benthic source (Figs. 5 and S2A–C). Sedimentary CH_4 is typically generated during microbial organic matter diagenesis and enters the overlying water column via diffusion and/or advective porewater exchange (Reeburgh, 2007; Sun et al., 2018). In addition, particularly in the EJS, pockmarks documented elsewhere on the seafloor, associated with gas-hydrate decomposition and/or bubble emission (Ruppel and Kessler, 2017), provide independent evidence of active sedimentary CH_4 release in this region. For example, Chun et al. (2012) reported dissolved CH_4 concentrations up to 40 nM directly above such geological features on the southern EJS shelf, attributing these elevated levels to diffusive sedimentary inputs. The bottom-water concentrations observed in this study are consistent with—though not definitive proof of—a similar sedimentary source and are broadly typical of continental shelf settings that receive high organic matter loading from both primary production and riverine supply (Reeburgh, 2007; Steinle et al., 2017).

https://doi.org/10.5194/egusphere-2026-6718
Preprint. Discussion started: 16 November 2026
© Author(s) 2026. CC BY 4.0 License.

The progressive decline in CH_4 concentrations from bottom water toward the mixed layer at most stations (Figs. 5 and S2A–C) indicates that sediment-derived CH_4 is substantially attenuated by dilution and/or microbial oxidation before reaching the surface, thereby limiting the direct contribution of this benthic source to sea–air CH_4 flux (Joung et al., 2022).

3.3 Subsurface CH_4 maximum: in situ production versus lateral transport

At stations deeper than ~300 m, a subsurface CH_4 maximum occurred within the thermocline (~90–130 m) in both the southwestern EJS and Ulleung Basin (Figs. 5B and 6), well above the seafloor and therefore not attributable to direct sedimentary diffusion. We consider two candidate sources: in situ water-column production and lateral advection from the shelf.

The subsurface CH_4 maximum coincided with a dissolved oxygen (DO) minimum (DO saturation as low as 50%; Figs. 6, S3 and S4), consistent with organic matter diagenesis, and with an increase in total bacterial abundance (16S rRNA gene copy number) at the same depth in both basins (Fig. 6). While this proxy does not resolve methanogen-specific activity, the co-occurring biomass increase is consistent with enhanced microbial metabolism within this layer. Previously, Gamo et al. (2012) also observed a subsurface maximum at sites similar to our study regions in the Ulleung Basin. They suggested that the elevation of CH_4 in that depth was attributed to anaerobic microenvironments of sinking particles (e.g., fecal pellets) by examining depleted $\delta^{13}C$ in CH_4 relative to particulate matter. In addition, Lee et al. (2018) reported a subsurface CH_4 maximum of up to 8.5 nM in the Gunsan Basin in Yellow Sea—a setting similar to our southwestern EJS stations—via the same mechanism. In fact, in the Ulleung Basin, bacterial abundance in June was more than fivefold higher than in March (Figs. 7A and C), coincident with the higher chlorophyll a typically reported for that season (Kwak et al., 2013a, b). This seasonal decoupling suggests that stratification-driven organic matter accumulation during summer enhances microbial decomposition, thereby promoting subsurface CH_4 production and its subsequent upward flux to the surface layer.

https://doi.org/10.5194/egusphere-2026-6718
Preprint. Discussion started: 16 November 2026
© Author(s) 2026. CC BY 4.0 License.

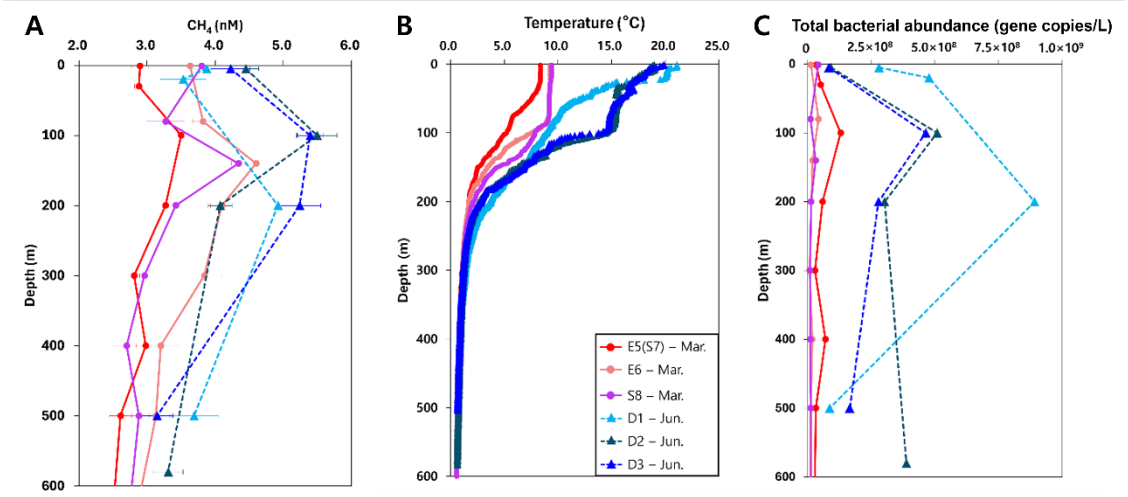


Figure 7. Vertical distributions of dissolved methane (CH_4) concentration, temperature, and total bacterial abundance in the Ulleung Basin in March and June 2025. Red and blue lines denote March and June 2025, respectively. Panels (A–C) show the vertical profiles of CH_4, temperature, and total bacterial abundance, respectively, at representative stations from the surface to 600 m depth.

Lateral advection from the adjacent shelf is also a plausible mechanism. Elevated CH_4 concentrations recurred within a consistent density range across surveys (σ_0 = 25.7–27.0 in 2023; σ_0 = 26.0–27.2 in 2024), consistent with isopycnal transport (Fig. S3). During the October 2025 cruise, the shelf-most station (Stn. pp1) showed a CH_4 plume of 48.7 nM at 60 m depth (~15 m above the seafloor), which decreased offshore toward pp5. This pattern is consistent with-though not conclusive proof of-lateral dispersion along the $\sigma_0 \approx 26.5$ isopycnal (Fig. 8). We note that, although this lateral advection trend was observed only in a transect from the shore to the Ulleung Basin, the advective flow could also likely occur in the shelf regions as well, particularly at the edge of the shelf break where abrupt depth changes occur, as is characteristic of settings in the southwestern EJS. For example, Brooks et al. (1981) and Joung et al. (2025) found subsurface CH_4 elevation at the edge of the shelf break in the northern Gulf of Mexico; they suggested that shelf currents at the break bring the sedimentary CH_4 offshore along the similar density. Moreover, this lateral transport has been reported in various marine environments, including the Spitsbergen shelf (Damm et al., 2005), the Tatar Strait of the northern EJS (Kholmogorov et al., 2023), and the Okinawa Trough shelf–slope transition (Toki et al., 2023). Consequently, this lateral transport is a ubiquitous process occurring in many shelf-break systems, and it would also occur in the southwestern EJS, where a sudden water depth change is apparent.

https://doi.org/10.5194/egusphere-2026-6718
Preprint. Discussion started: 16 November 2026
© Author(s) 2026. CC BY 4.0 License.

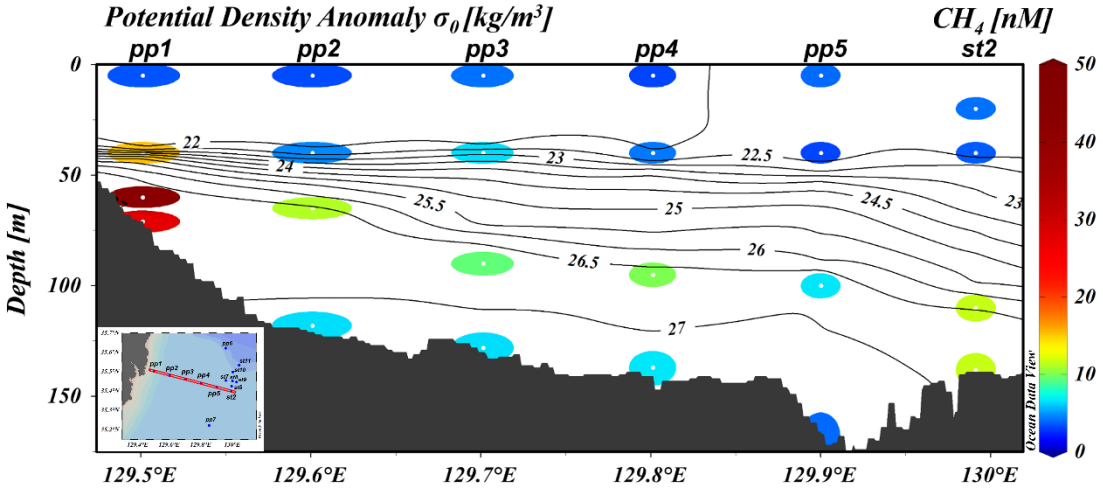


Figure 8. Vertical distribution of dissolved methane (CH_4) concentration along the coastal-to-offshore transect in the southwestern East (Japan) Sea in October 2025, with potential density anomaly (σ_0) contours overlaid.

Taken together, the subsurface CH_4 maximum most likely reflects a combination of in situ microbial production and lateral advection from the shelf, rather than either process acting alone. We note, however, that our interpretation is constrained by the absence of CH_4 stable-isotope data, nutrient and methylphosphonate measurements, and methanogen-specific microbial assays in this study, any of which would help partition source contributions more rigorously. In addition, the sampling transect was not designed explicitly to resolve transport pathways. Therefore, future studies in this system pairing CH_4 concentration measurements with $\delta^{13}C$-CH_4, nutrient/organic-phosphorus analysis, and targeted methanogen/methanotroph assays along isopycnal surfaces would help resolve the subsurface CH_4 maximum.

Relevant to the lateral transport, the decline in CH_4 concentration was substantial, decreasing from 48.7 to 6.6 nM (86% reduction; Fig. S5A). To evaluate the contribution of oxidation to the CH_4 decline along the pp1–pp5 transect (~37 km), we applied published oxidation rate constants (0.01–0.15 d^{-1}; Reeburgh, 2007; Steinle et al., 2017) to an estimated 8.6-day transit time (based on a current speed of 5 cm s^{-1}; Park et al., 2016). This yields an oxidative loss of up to 35.5 nM, leaving a predicted residual concentration of ~13.2 nM, which is still roughly twice the observed value of 6.6 nM (Fig. S5B). This gap suggests that oxidation alone underpredicts the observed attenuation, and that additional processes—such as mixing with CH_4-depleted water, variability in the transport pathway, and lateral dispersion (Mau et al., 2007, 2012)—likely contribute to the remaining concentration decrease.

Below the subsurface maximum in the Ulleung Basin, CH_4 declined with depth to below 3 nM beyond 1000 m (Figs. 6B and E), indicating that the microbial oxidation and/or mixing with CH_4-depleted deep water outcompetes any deep production at these depths (Gamo et al., 2012; Vereshchagina et al., 2013). Additionally, this study site harbors numerous gas hydrates at the seafloor (Chun et al., 2012), and thus our observations of CH_4 concentration below sea-air equilibrium suggest

https://doi.org/10.5194/egusphere-2026-6718
Preprint. Discussion started: 16 November 2026
© Author(s) 2026. CC BY 4.0 License.

only a minimal gas-hydrate contribution at these depths. This is consistent with Joung et al. (2022), who found that CH_4 sourced from gas hydrates below 500 m in the Ulleung Basin does not reach the surface, implying efficient removal of deep-sourced CH_4 during upward transport.

3.4 Sea-to-air CH_4 flux

The southwestern EJS and the Ulleung Basin were both predominantly net sources of CH_4 to the atmosphere, with fluxes remaining positive at the majority of stations across all sampling periods. Atmospheric CH_4 fluxes exhibited distinct seasonal variations at both sites. The October 2025 flux in the southwestern EJS was more than threefold higher than that in the other two surveys (Figs. S6A–C), coinciding with the highest surface CH_4 saturation and elevated wind speeds (Figs. S1H–I; Table S5), which aligns with a combined solubility/gas-transfer control. However, in the Ulleung Basin, the June flux was more than threefold higher than that in March (Figs. S6D and E), despite the lower wind speeds observed in June. This decoupling from wind speed indicates that sea surface temperature (via solubility) exerts a stronger seasonal control on the flux than wind alone, and that elevated summer temperatures and CH_4 saturation can sustain large fluxes even under comparatively weak winds.

Our Ulleung Basin fluxes (2.7 ± 2.5 μmol m^{-2} d^{-1}) are comparable to previously reported values for the northern East Sea (0.7 ± 1.0 μmol m^{-2} d^{-1}; Vereshchagina et al., 2013) and the major eastern basins (2.6 ± 1.9 μmol m^{-2} d^{-1}; Gamo et al., 2012), whereas coastal fluxes in the southwestern EJS are notably higher, particularly in October (Table S5), though this comparison spans studies that differ in sampling season, wind-speed data, and gas-transfer parameterization, and was not evaluated statistically. Scaling the average flux across this study and prior work (including eastern, Gamo et al., 2012; northern, Vereshchagina et al., 2013) (5.2 ± 6.4 μmol m^{-2} d^{-1}) to the entire EJS (~1×10^6 km^2) yields an estimated annual emission of 1.90×10^9 mol yr^{-1} (0.03 Tg CH_4 yr^{-1}) (Fig. 9). This is approximately 0.1–0.6% of estimated global ocean CH_4 emissions (5–25 Tg CH_4 yr^{-1}; Saunois et al., 2016), which is consistent with the EJS's share of global ocean area (~0.27%). We emphasize that this agreement is a plausibility check on the scaling arithmetic rather than an independent validation of the flux estimate itself, since the same area-weighted mean flux underlies both the EJS emission estimate and the percentage comparison to the global budget.

https://doi.org/10.5194/egusphere-2026-6718
Preprint. Discussion started: 16 November 2026
© Author(s) 2026. CC BY 4.0 License.

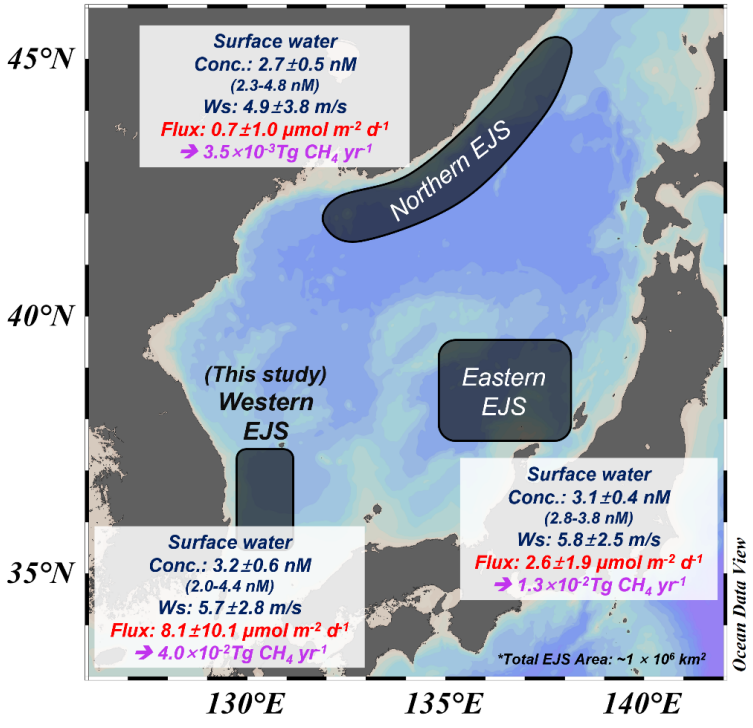


Figure 9. Comparison of surface water CH_4 parameters and sea-to-air flux estimates across sub-regions of the EJS. Map showing mean (±SD, with ranges in parentheses) surface CH_4 concentration (nM), wind speed (W_s, m s^{-1}), sea-to-air flux (μmol m^{-2} d^{-1}), and estimated annual emission (Tg CH_4 yr^{-1}) in the Northern EJS (Vereshchagina et al., 2013), Eastern EJS (Gamo et al., 2012), and Western EJS (this study). Values in each region are synthesized from published literature and current findings to scale regional emissions to the total area of the EJS (~1 × 10^6 km^2).

When comparing these values against other systems, the CH_4 fluxes in this study were broadly similar to open-ocean values (Table S5), suggesting that under most conditions, the EJS behaves more like an open-ocean CH_4 source than a seepage- or river-dominated shelf system, with episodic exceptions during strong stratification/high-temperature periods. For example, regions with extensive seafloor seepage, such as the northern Black Sea and northern Gulf of Mexico, show elevated water-column CH_4 and correspondingly high sea-to-air fluxes, although flux magnitudes vary considerably depending on the heterogeneous distribution of seep sites and differences in mixing intensity and microbial oxidation efficiency (Solomon et al., 2009; Hu et al., 2012). In the Black Sea specifically, strong stratification and a thick anoxic layer limit water-column oxidation of seafloor-derived CH_4 before it reaches the surface, favoring efficient atmospheric release (Amouroux et al., 2002). Instead, shallow shelf systems such as the Yellow Sea and East China Sea instead show high saturation and flux driven by the combined effects of seasonal riverine CH_4 input, temperature-enhanced biological production, and active benthic release (Yang et al., 2010; Lee et al., 2018).

https://doi.org/10.5194/egusphere-2026-6718
Preprint. Discussion started: 16 November 2026
© Author(s) 2026. CC BY 4.0 License.

We must note, however, that these flux estimates derive from spatiotemporally limited sampling and a simple linear extrapolation, and likely do not capture the full variability of actual regional emissions. Flux estimates based on climatological wind fields can also exceed in-situ measurement-based estimates by more than 50% (Morell et al., 2001), adding further uncertainty to any basin-scale budget built on reanalysis winds. Given that the largest fluxes we observed occurred during high-temperature, strongly stratified conditions, the EJS's CH_4 emission may be disproportionately sensitive to summer warming and stratification intensity under continued climate change. Sustained, high-resolution, in-situ flux observations, rather than periodic snapshot surveys, will be necessary to constrain the EJS CH_4 budget with confidence and to identify any long-term trend driven by regional warming. We also note that, because each cruise represents a single snapshot within its season, our dataset cannot resolve tidal-, diel- or storm-driven variability in CH_4 concentration or flux, and the seasonal comparisons above should be interpreted with this limitation in mind.

3.5 Monitoring the Donghae gas field as potential use in carbon storage

Several of our sampling stations in our survey lie within the Donghae gas field, a natural gas (predominantly CH_4) production site that ceased operation in 2021 and is now under consideration for CO_2 capture and storage (CCS; Park et al., 2024). Ki et al. (2022) provide a comprehensive review of the field's exploration, development, and production history and its potential for CO_2 storage and utilization. Because the seafloor in this region also hosts pockmarks indicative of past or ongoing gas migration, establishing whether the depleted reservoir currently shows any detectable CH_4 anomaly is a necessary step before the site can be monitored for CO_2 leakage during and after storage operations.

Mean CH_4 concentrations at the gas-field stations fell within the range observed outside the gas field in every survey, with the two groups' distributions overlapping throughout. Because the gas-field group comprised as few as two stations in some surveys (e.g., 2024) and the outside-group values in 2025 were strongly influenced by a single high observation (28.2 nM), we do not treat this as a statistically tested comparison. Within that limitation, this five-survey dataset shows no concentration pattern that distinguishes the gas-field stations from their surroundings; this should be read as an indicative baseline rather than a confirmed absence of anomaly, and does not rule out a small or spatially localized CH_4 signal that the current station density and sample sizes are not positioned to detect.

Because these observations were collected during a period of platform inactivity and prior to any CO_2 injection, they constitute a useful pre-storage CH_4 baseline for the site. Any future deviation from the concentration range and spatial patterns documented here (7–10 nM at gas-field stations, broadly consistent with regional background) would thus provide a meaningful reference point against which to evaluate potential leakage once CCS operations begin. Continued monitoring at this frequency, ideally with expanded spatial coverage within the gas field, would strengthen the baseline and support early detection of any future anomaly. We caution that, with only a small number of stations located directly within the gas field, the present station density may not be sufficient to detect a spatially localized leak, and natural small-scale heterogeneity in CH_4 could mask a modest, early-stage anomaly. We have not performed a formal statistical power analysis to quantify the

https://doi.org/10.5194/egusphere-2026-6718
Preprint. Discussion started: 16 November 2026
© Author(s) 2026. CC BY 4.0 License.

minimum leak magnitude our current sampling design could reliably detect against natural background variability. Natural geologic events such as earthquakes could also independently trigger or reactivate leakage pathways—a risk that has not been assessed for this site. We recommend that both a quantitative detection threshold and a site-specific seismic-hazard assessment be established, alongside continued baseline monitoring, before CCS operations begin.

4 Conclusions

We present the vertical distribution of dissolved CH_4 in the southwestern and the Ulleung Basin in the East (Japan) Sea (EJS) and assess the sea-to-air CH_4 flux to evaluate the region's contribution to atmospheric CH_4. In the southwestern EJS, CH_4 concentrations generally peaked in the bottom waters, likely reflecting benthic CH_4 inputs driven by the microbial degradation of organic matter in sediments. Meanwhile, at certain stations, a subsurface CH_4 maximum was observed. This is potentially attributable to a combination of aerobic in situ CH_4 production and the horizontal diffusion or transport of sedimentary CH_4 from the coast. Most of the high CH_4 at the bottom layer was removed before reaching the surface, maintaining low concentrations in the surface waters. Surface waters of the EJS were supersaturated with CH_4 relative to the atmosphere, acting as a net atmospheric source. The CH_4 fluxes exhibited significant seasonal variability, driven by a complex combination of changes in CH_4 concentration, solubility, and wind speeds. Based on an average flux of 5.2 ± 6.4 μmol m^{-2} d^{-1} obtained from both this and previous studies, annual CH_4 emissions from the EJS are estimated at ~0.03 Tg CH_4 yr^{-1}. This accounts for approximately 0.1–0.6% of global ocean CH_4 emissions (5–25 Tg CH_4 yr^{-1}), which is consistent with the EJS's share of global ocean area (~0.27%). As in the Results, we note this area-share comparison reflects the same scaling assumptions used to derive the emission estimate itself, rather than an independent confirmation of it. While EJS CH_4 fluxes are generally comparable to open-ocean levels, sharp seasonal increases in June demonstrate the region's potential for significant episodic emissions. However, as these estimates are based on spatiotemporally limited data, they may not fully capture the annual emission budget of the entire EJS. Therefore, continuous observations with higher spatiotemporal resolution are necessary for a more precise quantification. Furthermore, future investigations aimed at identifying CH_4 sources and sinks are required to fully elucidate the biogeochemical cycling of CH_4 in the EJS.

https://doi.org/10.5194/egusphere-2026-6718
Preprint. Discussion started: 16 November 2026
© Author(s) 2026. CC BY 4.0 License.

Code and data availability

All data are available upon request to the corresponding author.

Supplement Information

The supplement file is provided online as separate file

Author contributions

DJJ designed the study. JYL conducted the field observations and sample collection, with support from ITK as the chief scientist during the research cruise. JYL performed the methane laboratory experiments and data analyses under the supervision of DJJ. SRB performed the bacterial sample analyses and EHL supervised the analysis and data provision. BKK, JHL, and DSH contributed to data interpretation and provided constructive feedback. JYL and DJJ wrote the main manuscript, and all authors contributed to reviewing and approving the final manuscript.

Competing interests

The authors declare that they have no conflict of interests.

Acknowledgements

We would like to thank all lab members for their assistance. We also express our gratitude to the captains and crews of the research vessels (R/V *Onnuri*, R/V *Isabu*, R/V *Dokdonuri*, and R/V *Eardo*) for their support during the sampling cruises at sea. During the preparation of this manuscript, the corresponding author used Claude (Anthropic) to assist with language editing and verifying the reference list. After using this tool, the authors reviewed and edited the content as needed and take full responsibility for the content of the published article.

Financial support

This research was supported by Global - Learning & Academic research institution for Master's·PhD students, and Postdocs(G-LAMP) Program of the National Research Foundation of Korea (NRF) grant funded by the Ministry of Education(No. RS-2023-00301938). DH was partially supported by KIMST funded by the Ministry of Oceans and Fisheries (RS-2023–00254680) and the NRF grant (RS-2024-00348973), funded by the Korea government (MSIT).

https://doi.org/10.5194/egusphere-2026-6718
Preprint. Discussion started: 16 November 2026
© Author(s) 2026. CC BY 4.0 License.

Review statement

The review statement will be added by Copernicus Publications listing the handling editor as well as all contributing referees according to their status anonymous or identified.

References

Amouroux, D., Roberts, G., Rapsomanikis, S., and Andreae, M. O.: Biogenic gas (CH_4, N_2O, DMS) emission to the atmosphere from near-shore and shelf waters of the northwestern Black Sea, Estuar. Coast. Shelf Sci., 54, 575–587, https://doi.org/10.1006/ecss.2000.0666, 2002

Bange, H. W., Bartell, U. H., Rapsomanikis, S., and Andreae, M. O.: Methane in the Baltic and North Seas and a reassessment of the marine emissions of methane, Global Biogeochem. Cycles, 8, 465–480, https://doi.org/10.1029/94GB02181, 1994.

Bange, H. W., Bergmann, K., Hansen, H. P., Kock, A., Koppe, R., Malien, F., and Ostrau, C.: Dissolved methane during hypoxic events at the Boknis Eck time series station (Eckernförde Bay, SW Baltic Sea), Biogeosciences, 7, 1279–1284, https://doi.org/10.5194/bg-7-1279-2010, 2010.

Bates, T. S., Kelly, K. C., Johnson, J. E., and Gammon, R. H.: A reevaluation of the open ocean source of methane to the atmosphere, J. Geophys. Res.-Atmos., 101, 6953–6961, https://doi.org/10.1029/95JD03348, 1996.

Borges, A. V., Champenois, W., Gypens, N., Delille, B., and Harlay, J.: Massive marine methane emissions from near-shore shallow coastal areas, Sci. Rep., 6, 27908, https://doi.org/10.1038/srep27908, 2016.

Breitburg, D., Levin, L. A., Oschlies, A., Grégoire, M., Chavez, F. P., Conley, D. J., Garçon, V., Gilbert, D., Gutiérrez, D., Isensee, K., Jacinto, G. S., Limburg, K. E., Montes, I., Naqvi, S. W. A., Pitcher, G. C., Rabalais, N. N., Roman, M. R., Rose, K. A., Seibel, B. A., Telszewski, M., Yasuhara, M., and Zhang, J.: Declining oxygen in the global ocean and coastal waters, Science, 359, eaam7240, https://doi.org/10.1126/science.aam7240, 2018.

Brooks, J. M., Reid, D. F., and Bernard, B. B.: Methane in the upper water column of the northwestern Gulf of Mexico, J. Geophys. Res.-Oceans, 86, 11029–11040, https://doi.org/10.1029/JC086iC11p11029, 1981.

Byun, S. K. and Chang, S. D.: Two branches of Tsushima Warm Current in the western channel of the Korea Strait, J. Oceanol. Soc. Korea, 19, 200–209, 1984.

Chang, K. I., Teague, W. J., Lyu, S. J., Perkins, H. T., Lee, D. K., Watts, D. R., Kim, K., Mitchell, D. A., Lee, J. H., and Kim, K.: Circulation and currents in the southwestern East/Japan Sea: overview and review, Prog. Oceanogr., 61, 105–156, https://doi.org/10.1016/j.pocean.2004.06.005, 2004.

Chun, J. H., Ryu, B. J., Lee, C. S., Park, K. P., Yoo, D. G., and Kim, G. Y.: Factors determining the spatial distribution of gas-charged sediments in the continental shelf off southeastern Korea, Mar. Geol., 332, 27–39, https://doi.org/10.1016/j.margeo.2012.06.004, 2012.

https://doi.org/10.5194/egusphere-2026-6718
Preprint. Discussion started: 16 November 2026
© Author(s) 2026. CC BY 4.0 License.

Chun, J. H., Kim, Y., Bahk, J. J., Kim, S. P., and Lee, S. H.: Late Holocene distal mud deposits off the Nakdong delta, SE Korea: evidence for shore-parallel sediment transport in a current-dominated setting, Geo-Mar. Lett., 35, 475–485, https://doi.org/10.1007/s00367-015-0419-1, 2015.

Cole, J. J. and Caraco, N. F.: Atmospheric exchange of carbon dioxide in a low-wind oligotrophic lake measured by the addition of SF_6, Limnol. Oceanogr., 43, 647–656, https://doi.org/ 10.4319/lo.1998.43.4.0647, 1998.

Damm, E., Mackensen, A., Budéus, G., Faber, E., and Vinogradov, S. M.: Pathways of methane in seawater: plume spreading in an Arctic shelf environment (SW-Spitsbergen), Cont. Shelf Res., 25, 1453–1472, https://doi.org/10.1016/j.csr.2005.03.003, 2005.

Gamo, T., Tsunogai, U., Hirota, A., Nakagawa, F., Zilberman, E. V., and Obata, H.: First measurements of methane and its carbon isotope ratio in the Japan Sea (East Sea), Mar. Chem., 128, 92–99, https://doi.org/10.1016/j.marchem.2011.10.006, 2012.

Gelesh, L., Marshall, K., Boicourt, W., and Lapham, L.: Methane concentrations increase in bottom waters during summertime anoxia in the highly eutrophic estuary, Chesapeake Bay, USA, Limnol. Oceanogr., 61, S253–S266, https://doi.org/ 10.1002/lno.10272, 2016.

Hamdan, L. J. and Wickland, K. P.: Methane emissions from oceans, coasts, and freshwater habitats: new perspectives and feedbacks on climate, Limnol. Oceanogr., 61, S3–S12, https://doi.org/10.1002/lno.10449, 2016.

Hu, L., Yvon-Lewis, S. A., Kessler, J. D., and MacDonald, I. R.: Methane fluxes to the atmosphere from deepwater hydrocarbon seeps in the northern Gulf of Mexico, J. Geophys. Res.-Oceans, 117, C00H09, https://doi.org/10.1029/2011JC007208, 2012.

Huh, S., Yoo, H. S., Kim, H. J., Lee, G. H., and Kim, C. S.: A study on the characteristics of gas hydrate layer distributed in the southern area of the Ulleung Basin, East Sea, Korean J. Pet. Geol., 10, 18–22, 2004.

IPCC: Climate Change 2021: The Physical Science Basis. Contribution of Working Group I to the Sixth Assessment Report of the Intergovernmental Panel on Climate Change, edited by: Masson-Delmotte, V., Zhai, P., Pirani, A., Connors, S. L., Péan, C., Berger, S., Caud, N., Chen, Y., Goldfarb, L., Gomis, M. I., Huang, M., Leitzell, K., Lonnoy, E., Matthews, J. B. R., Maycock, T. K., Waterfield, T., Yelekçi, O., Yu, R., and Zhou, B., Cambridge University Press, Cambridge, United Kingdom and New York, NY, USA, 2391 pp., https://doi.org/10.1017/9781009157896, 2021.

Jeong, S. Y. and Kim, T. G.: Effects of dispersal on species distribution, abundance, diversity and interaction in a bacterial biofilm metacommunity, J. Appl. Microbiol., 132, 459–469, https://doi.org/10.1111/jam.15194, 2022.

Joung, D., Ruppel, C., Southon, J., Kessler, J. D., and Weber, T.: Negligible atmospheric release of methane from decomposing hydrates in mid-latitude oceans, Nat. Geosci., 15, 885–891, https://doi.org/10.1038/s41561-022-01044-6, 2022.

Joung, D., Weber, T., Gregory, K., Chanton, J. P., and Joye, S. B.: Deep Gulf of Mexico seeps are not a significant source of methane to the atmosphere, Commun. Earth Environ., 6, 999, https://doi.org/10.1038/s43247-025-00000-0, 2025.

https://doi.org/10.5194/egusphere-2026-6718
Preprint. Discussion started: 16 November 2026
© Author(s) 2026. CC BY 4.0 License.

Jung, M., Koirala, S., Weber, U., Ichii, K., Gans, F., Camps-Valls, G., Papale, D., Schwalm, C., Tramontana, G., and Reichstein, M.: The FLUXCOM ensemble of global land-atmosphere energy fluxes, Sci. Data, 6, 74, https://doi.org/10.1038/s41597-019-0076-8, 2019.

Karl, D. M. and Tilbrook, B. D.: Production and transport of methane in oceanic particulate organic matter, Nature, 368, 732–734, https://doi.org/10.1038/368732a0, 1994.

Karl, D. M., Beversdorf, L., Björkman, K. M., Church, M. J., Martinez, A., and DeLong, E. F.: Aerobic production of methane in the sea, Nat. Geosci., 1, 473–478, https://doi.org/10.1038/ngeo234, 2008.

Kastner, M.: Gas hydrates in convergent margins: formation, occurrence, geochemistry, and global significance, in: Natural Gas Hydrates: Occurrence, Distribution, and Detection, Geophys. Monogr. Ser., vol. 124, edited by: Paull, C. K. and Dillon, W. P., AGU, Washington, D. C., 67–86, https://doi.org/10.1029/GM124p0067, 2001.

Ki, S., Back, S., Bae, K., Kim, J., and Lee, H.: Donghae-1 gas field development and its application to CCS, J. Korean Soc. Miner. Energy Resour. Eng., 59, 498–517, https://doi.org/10.32390/ksmer.2022.59.5.498, 2022.

Kholmogorov, A., Ponomarev, V., Syrbu, N., and Shkorba, S.: Dissolved methane transport in the Tatar Strait and the deepest basin of the Japan (East) Sea from its possible sources, Water, 15, 821, https://doi.org/10.3390/w15040821, 2023.

Kim, D., Choi, J. G., Park, J., Kim, C. S., and Cho, Y. K.: Upwelling processes driven by contributions from wind and current in the southwest East Sea (Japan Sea), Front. Mar. Sci., 10, 1165366, https://doi.org/10.3389/fmars.2023.1165366, 2023.

Kim, D. S., Choi, M. S., Oh, H. Y., Kim, K. H., and Kim, K. R.: Estimation of particulate organic carbon flux in the southwestern East Sea during summer using $^{234}Th/^{238}U$ disequilibrium, The Sea, 14, 1–9, 2009.

Kim, K., Kim, K. R., Kim, Y. G., Cho, Y. K., Kang, D. J., Takematsu, M., Volkov, Y., and Yoon, J. H.: Water masses and decadal variability in the East Sea (Sea of Japan), Prog. Oceanogr., 61, 157–174, https://doi.org/10.1016/j.pocean.2004.06.003, 2004.

Kwak, J. H., Hwang, J., Choy, E. J., Park, H. J., Kang, D. J., Suh, Y. S., and Kang, C. K.: High primary productivity and f-ratio in summer in the Ulleung Basin of the East/Japan Sea, Deep-Sea Res. Pt. I, 79, 74–85, https://doi.org/10.1016/j.dsr.2013.05.011, 2013a.

Kwak, J. H., Lee, S. H., Park, H. J., Choy, E. J., Jeong, H. D., Kim, K. R., and Kang, C. K.: Monthly measured primary and new productivities in the Ulleung Basin as a biological "hot spot" in the East/Japan Sea, Biogeosciences, 10, 4405–4417, https://doi.org/10.5194/bg-10-4405-2013, 2013b.

Kwon, T. H., Lee, K. R., Cho, G. C., and Lee, J. Y.: Geotechnical properties of deep oceanic sediments recovered from the hydrate occurrence regions in the Ulleung Basin, East Sea, offshore Korea, Mar. Pet. Geol., 28, 1870–1883, https://doi.org/10.1016/j.marpetgeo.2011.02.003, 2011.

Lan, X., Tans, P., and Thoning, K. W.: Trends in globally-averaged CO_2 determined from NOAA Global Monitoring Laboratory measurements, Version 05-Dec-2025, NOAA Global Monitoring Laboratory [data set], https://doi.org/10.15138/9N0H-ZH07, 2025a.

https://doi.org/10.5194/egusphere-2026-6718
Preprint. Discussion started: 16 November 2026
© Author(s) 2026. CC BY 4.0 License.

Lan, X., Thoning, K. W., and Dlugokencky, E. J.: Trends in globally-averaged CH_4, N_2O, and SF_6 determined from NOAA Global Monitoring Laboratory measurements, Version 2025-12, NOAA Global Monitoring Laboratory [data set], https://doi.org/10.15138/P8XG-AA10, 2025b.

Lashof, D. A. and Ahuja, D. R.: Relative contributions of greenhouse gas emissions to global warming, Nature, 344, 529–531, https://doi.org/ 10.1038/344529a00, 1990.

Lee, C. H., Lim, Y. K., Kim, M., Park, J. S., and Lee, J. H.: Seasonal phytoplankton characteristics related with region-specific coastal environments in the Korean Peninsula, J. Mar. Sci. Eng., 12, 1008, https://doi.org/10.3390/jmse12061008, 2024.

Lee, D. S. and Rho, T. K.: N:P ratio in the East Sea, The Sea, 20, 199–205, https://doi.org/10.7850/jkso.2015.20.4.199, 2015.

Lee, H., Zhumabieke, M., Jeon, G. U., Kim, J., and Park, J. H.: Differential river-to-sea transfers and CH_4 dominance of greenhouse gas emissions in urbanized and impounded estuaries, Sci. Total Environ., 978, 179444, https://doi.org/10.1016/j.scitotenv.2025.179444, 2025.

Lee, J. H., Woo, H. J., Son, S. K., Kim, Y. H., and Kang, D. J.: Flux and distribution of methane CH_4) in the Gunsan Basin of the southeastern Yellow Sea, off western Korea, J. Environ. Sci. Health A, 53, 457–466, https://doi.org/10.1080/10934529.2017.1409026, 2018.

Lee, Y. W., Park, M. O., Kim, S. G., and Choi, Y. S.: Long-term variations in pH in coastal waters along the Korean Peninsula, Biogeosciences, 22, 675–690, https://doi.org/10.5194/bg-22-675-2025, 2025.

Leonte, M., Wang, B., Socolofsky, S. A., Mau, S., Breier, J. A., and Kessler, J. D.: Using carbon isotope fractionation to constrain the extent of methane dissolution into the water column surrounding a natural hydrocarbon gas seep in the northern Gulf of Mexico, Geochem. Geophys. Geosyst., 19, 4459–4475, https://doi.org/10.1029/2018GC007705, 2018.

Mau, S., Valentine, D. L., Clark, J. F., Reed, A. R., Camilli, R., and Washburn, L.: Dissolved methane distributions and air-sea flux in the plume of a massive seep field, Coal Oil Point, California, Geophys. Res. Lett., 34, L22603, https://doi.org/10.1029/2007GL031344, 2007.

Mau, S., Heintz, M. B., and Valentine, D. L.: Quantification of CH_4 loss and transport in dissolved plumes of the Santa Barbara Channel, California, Cont. Shelf Res., 32, 110–120, https://doi.org/10.1016/j.csr.2011.10.016, 2012.

Morell, J. M., Capella, J., Mercado, A., Bauzá, J., and Corredor, J. E.: Nitrous oxide fluxes in Caribbean and tropical Atlantic waters: evidence for near surface production, Mar. Chem., 74, 131–143, https://doi.org/10.1016/S0304-4203(01)00011-1, 2001.

National Institute of Meteorological Sciences: Global Atmosphere Watch Report 2024, National Institute of Meteorological Sciences, Available from: http://www.climate.go.kr/home/bbs/view.php?code=24&bname=report&vcode=7052, 2024.

Park, I. S., Park, S. H., Park, S. H., and Cha, S. H.: CCS demonstration research using depleted gas fields in the East Sea, Proc. Korean Soc. Clim. Change Res., 91, 2024.

Park, J. H., Chang, K. I., and Nam, S.: Summertime coastal current reversal opposing offshore forcing and local wind near the middle east coast of Korea: observation and dynamics, Geophys. Res. Lett., 43, 7097–7105, https://doi.org/10.1002/2016GL069322, 2016.

https://doi.org/10.5194/egusphere-2026-6718
Preprint. Discussion started: 16 November 2026
© Author(s) 2026. CC BY 4.0 License.

Rabalais, N. N., Turner, R. E., Wiseman, W. J. Jr., and Boesch, D. F.: A brief summary of hypoxia on the northern Gulf of Mexico continental shelf: 1985–1988, Geol. Soc. Lond. Spec. Publ., 58, 35–47, https://doi.org/10.1144/GSL.SP.1991.058.01.03, 1991.

Reeburgh, W. S.: Oceanic methane biogeochemistry, Chem. Rev., 107, 486–513, https://doi.org/10.1021/cr050362v, 2007.

Repeta, D. J., Ferrón, S., Sosa, O. A., Johnson, C. G., Repeta, L. D., Arey, J. S., and Karl, D. M.: Marine methane paradox explained by bacterial degradation of dissolved organic matter, Nat. Geosci., 9, 884–887, https://doi.org/10.1038/ngeo2837, 2016.

Rhee, T. S., Kettle, A. J., and Andreae, M. O.: Methane and nitrous oxide emissions from the ocean: a reassessment using basin-wide observations in the Atlantic, J. Geophys. Res.-Atmos., 114, D12304, https://doi.org/10.1029/2008JD011662, 2009.

Ruppel, C. D. and Kessler, J. D.: The interaction of climate change and methane hydrates, Rev. Geophys., 55, 126–168, https://doi.org/10.1002/2016RG000534, 2017.

Saunois, M., Bousquet, P., Poulter, B., Peregon, A., Ciais, P., Canadell, J. G., Dlugokencky, E. J., Etiope, G., Bastviken, D., Houweling, S., Janssens-Maenhout, G., Tubiello, F. N., Castaldi, S., Jackson, R. B., Alexe, M., Arora, V. K., Beerling, D. J., Bergamaschi, P., Blake, D. R., Brailsford, G., Brovkin, V., Bruhwiler, L., Crevoisier, C., Feng, L., Frankenberg, C., Gedney, N., Hogan, L., Hopkins, A., Huang, M., Ito, A., Joos, F., Kim, H. S., Krummel, P. B., Lamarque, J. F., Lavenu, S., Levy, P., Loh, Z., Mak, S., Matsunaga, T., McKinley, G. A., Metzl, N., Miller, J. B., Nishioka, Y., O'Doherty, S., Parker, R., Peng, S., Pellegrini, M., Pison, I., Prigent, C., Prinn, R. G., Ramonet, M., Riley, W. J., Saito, M., Santini, M., Schroeder, R., Simpson, I. J., Spahni, R., Steele, P., Takizawa, A., Thornton, B. F., Tian, H., Tohjima, Y., Viovy, N., Voulgarakis, A., van Weele, M., van der Werf, G. R., Weiss, R., Wiedinmyer, C., Woolf, D., Young, D., Zheng, B., Zhu, Q., Zhu, Z., and Zhuang, Q.: The global methane budget: 2000–2012, Earth Syst. Sci. Data Discuss., 8, 697–751, https://doi.org/10.5194/essd-8-697-2016, 2016.

Saunois, M., Stavert, A. R., Poulter, B., Bousquet, P., Canadell, J. G., Jackson, R. B., Raymond, P. A., Dlugokencky, E. J., Houweling, S., Patra, P. K., Ciais, P., Arora, V. K., Bastviken, D., Bergamaschi, P., Blake, D. R., Brailsford, G., Bruhwiler, L., Carlson, K. M., Carrol, M., Castaldi, S., Chandra, N., Crevoisier, C., Crill, P. M., Covey, K., Curry, C. L., Etiope, G., Frankenberg, C., Gedney, N., Hegglin, M. I., Höglund-Isaksson, L., Hugelius, G., Ishizawa, M., Ito, A., Janssens-Maenhout, G., Jensen, K. M., Joos, F., Kleinen, T., Krummel, P. B., Langenfelds, R. L., Laruelle, G. G., Liu, L., Machida, T., Maksyutov, S., McDonald, K. C., McNorton, J., Miller, P. A., Melton, J. R., Morino, I., Müller, J., Murguia-Flores, F., Naik, V., Niwa, Y., Noojipady, P., Nguyen, M. C., Pan, S., Parker, R., Peters, G., Piscison, I., Plass-Dölmer, R., Prigent, C., Prinn, R. G., Ramonet, M., Regnier, P., Riley, W. J., Rosentreter, J. A., Segers, A., Simpson, I. J., Shi, H., Smith, S. J., Steele, L. P., Thornton, B. F., Tian, H., Tohjima, Y., Tubiello, F. N., Tsuruta, A., Viovy, N., Voulgarakis, A., Weber, T. S., van Weele, M., van der Werf, G. R., Weiss, R. F., Worthy, D., Wunch, D., Yin, Y., Yoshida, Y., Zhang, W., Zhang, Z., Zhao, Y., Zheng, B., Zhu, Q., Zhu, Q., and Zhuang, Q.: The global methane budget 2000–2017, Earth Syst. Sci. Data Discuss., 12, 1561–1623, https://doi.org/10.5194/essd-12-1561-2020, 2020.

Shim, M. J. and Yoon, Y. Y.: Long-term variation of nitrate in the East Sea, Korea, Environ. Monit. Assess., 193, 781, https://doi.org/10.1007/s10661-021-09425-z, 2021.

https://doi.org/10.5194/egusphere-2026-6718
Preprint. Discussion started: 16 November 2026
© Author(s) 2026. CC BY 4.0 License.

Soliman, T., Yang, S. Y., Yamazaki, T., and Jenke-Kodama, H.: Profiling soil microbial communities with next-generation sequencing: the influence of DNA kit selection and technician technical expertise, PeerJ, 5, e4178, https://doi.org/10.7717/peerj.4178, 2017.

Solomon, E. A., Kastner, M., MacDonald, I. R., and Leifer, I.: Considerable methane fluxes to the atmosphere from hydrocarbon seeps in the Gulf of Mexico, Nat. Geosci., 2, 561–565, https://doi.org/10.1038/ngeo574, 2009.

Steinle, L., Maltby, J., Treude, T., Ferdelman, T. G., Niemann, H., and Lehmann, M. F.: Effects of low oxygen concentrations on aerobic methane oxidation in seasonally hypoxic coastal waters, Biogeosciences, 14, 1631–1645, https://doi.org/10.5194/bg-14-1631-2017, 2017.

Stramma, L., Johnson, G. C., Sprintall, J., and Mohrholz, V.: Expanding oxygen-minimum zones in the tropical oceans, Science, 320, 655–658, https://doi.org/10.1126/science.1153847, 2008.

Sun, M. S., Zhang, G. L., Ma, X., Cao, X. X., Mao, H. B., Li, J., and Ye, W. W.: Dissolved methane in the East China Sea: distribution, seasonal variation and emission, Mar. Chem., 202, 12–26, https://doi.org/ 10.1016/j.marchem.2018.03.001, 2018.

Takata, H., Kuma, K., Isoda, Y., Kuroda, H., Takagi, F., Sakaoka, K., and Suzuki, K.: Iron in the Japan Sea and its implications for the physical processes in deep water, Geophys. Res. Lett., 35, L02607, https://doi.org/10.1029/2007GL031794, 2008.

Toki, T., Chibana, H., Shimabukuro, T., and Yamakawa, Y.: Distribution of dissolved methane in seawater from the East China Sea to the Ryukyu forearc, Front. Earth Sci., 11, 1174504, https://doi.org/10.3389/feart.2023.1174504, 2023.

Turner, R. E., Rabalais, N. N., and Justic, D.: Predicting summer hypoxia in the northern Gulf of Mexico: riverine N, P, and Si loading, Mar. Pollut. Bull., 52, 139–148, https://doi.org/10.1016/j.marpolbul.2005.08.012, 2006.

Upstill-Goddard, R. C., Rees, A. P., and Owens, N. J. P.: Simultaneous high-precision measurements of methane and nitrous oxide in water and seawater by single phase equilibration gas chromatography, Deep-Sea Res. Pt. I, 43, 1669–1682, https://doi.org/10.1016/S0967-0637(96)00074-X, 1996.

Valentine, D. L., Blanton, D. C., Reeburgh, W. S., and Kastner, M.: Water column methane oxidation adjacent to an area of active hydrate dissociation, Eel River Basin, Geochim. Cosmochim. Acta, 65, 2633–2640, https://doi.org/ 10.1016/S0016-7037(01)00625-1, 2001.

Vereshchagina, O. F., Korovitskaya, E. V., and Mishukova, G. I.: Methane in water columns and sediments of the northwestern Sea of Japan, Deep-Sea Res. Pt. II, 86, 25–33, https://doi.org/10.1016/j.dsr2.2012.08.003, 2013.

Wanninkhof, R.: Relationship between wind speed and gas exchange over the ocean, J. Geophys. Res.-Oceans, 97, 7373–7382, https://doi.org/10.1029/92JC00188, 1992.

Weinstein, A., Navarrete, L., Ruppel, C., Weber, T. C., Leonte, M., Kellermann, M. I., Arrington, E. C., and Kessler, J. D.: Determining the flux of methane into Hudson Canyon at the edge of methane clathrate hydrate stability, Geochem. Geophys. Geosyst., 17, 3882–3892, https://doi.org/10.1002/2016GC006421, 2016.

Wilson, S. T., Bange, H. W., Arévalo-Martínez, D. L., Barnes, J., Borges, A. V., Brown, I., Bullister, J. L., Burgos, M., Capelle, D. W., Casso, M., de la Paz, M., Farías, L., Fenwick, L., Ferrón, S., Garcia-Tigreros, F., Glockzin, M., Grundle, D. S., Gutekunst, S., Hamme, R. C., Heintz, M. B., Hirota, A., Hirota, M., Hu, L., Ilyina, T., Joung, D., Kock, A., Koerte, L., Kock,

https://doi.org/10.5194/egusphere-2026-6718
Preprint. Discussion started: 16 November 2026
© Author(s) 2026. CC BY 4.0 License.

A., Kuss, J., Lapham, L. L., Leonte, M., Lin, I., Mau, S., Miller, L. B., Naqvi, S. W. A., Nishino, S., Ocean, C., Owings, S. M., Park, S. H., Peiffer, S., Rehder, G., Retamal, L., Rhee, T. S., Robidoux, M. M., Santoro, A. E., Schlundt, C., Schmale, O., Socolofsky, S. A., Sosa, O. A., Sun, M. S., Tan, S. M., Tanhua, T., Upstill-Goddard, R. C., Valentine, D. L., Wanninkhof, R., Weber, T. S., Wilson, S., Wissel, H., Yang, J., Ye, W. W., Yvon-Lewis, S. A., Zhang, G. L., Zhang, J., and Zindler, C.: An intercomparison of oceanic methane and nitrous oxide measurements, Biogeosciences, 15, 5891–5907, https://doi.org/10.5194/bg-15-5891-2018, 2018.

Won, J. H. and Lee, Y. W.: Spatio-temporal variations of marine environmental characteristics in the southwestern East Sea, The Sea, 20, 16–28, https://doi.org/10.7850/jkso.2015.20.1.16, 2015.

Yang, J., Zhang, G. L., Zheng, L. X., Zhang, F., and Zhao, Y. C.: Seasonal variation of fluxes and distributions of dissolved methane in the North Yellow Sea, Cont. Shelf Res., 30, 187–192, https://doi.org/10.1016/j.csr.2009.10.016, 2010.

Ye, W. W., Wang, X. L., Zhang, X. H., and Zhang, G. L.: Methane production in oxic seawater of the western North Pacific and its marginal seas, Limnol. Oceanogr., 65, 2352–2365, https://doi.org/10.1002/lno.11457, 2020.

Zhang, G., Zhang, J., Liu, S., Ren, J., and Zhao, J.: Methane in the Changjiang (Yangtze River) estuary and its adjacent marine area: riverine input, sediment release and atmospheric fluxes, Biogeochemistry, 91, 71–84, https://doi.org/10.1007/s10533-008-9259-7, 2008.

Zindler, C., Bracher, A., Marandino, C. A., Taylor, B., Torrecilla, E., Kock, A., and Bange, H. W.: Sulphur compounds, methane, and phytoplankton: interactions along a north-south transit in the western Pacific Ocean, Biogeosciences, 10, 3297–3311, https://doi.org/10.5194/bg-10-3297-2013, 2013.

Żygadłowska, O. M., Roth, F., van Helmond, N. A., Slomp, C. P., and Hagens, M.: Eutrophication and deoxygenation drive high methane emissions from a brackish coastal system, Environ. Sci. Technol., 58, 10582–10590, https://doi.org/10.1021/acs.est.4c00702, 2024.